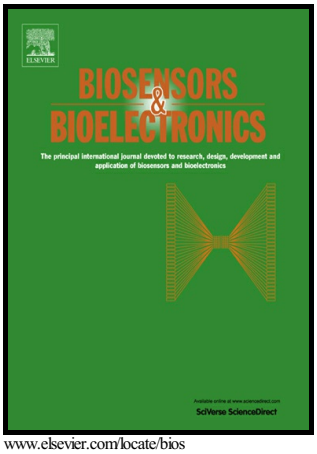

www.elsevier.com/locate/bios

Pyrrolidinyl PNA polypyrrole/silver nanofoam electrode as a novel label-free electrochemical miRNA-21 biosensor

Tawatchai Kangkamano, Apon Numnuam, Warakorn Limbut, Proespichaya Kanatharana, Tirayut Vilaivan, Panote Thavarungkul

PII: S0956-5663(17)30753-4
DOI: https://doi.org/10.1016/j.bios.2017.11.024
Reference: BIOS10100

To appear in: *Biosensors and Bioelectronic*

Received date: 11 September 2017
Revised date: 22 October 2017
Accepted date: 5 November 2017

Cite this article as: Tawatchai Kangkamano, Apon Numnuam, Warakorn Limbut, Proespichaya Kanatharana, Tirayut Vilaivan and Panote Thavarungkul, Pyrrolidinyl PNA polypyrrole/silver nanofoam electrode as a novel label-free electrochemical miRNA-21 biosensor, *Biosensors and Bioelectronic,* https://doi.org/10.1016/j.bios.2017.11.024

Pyrrolidinyl PNA polypyrrole/silver nanofoam electrode as a novel label-free electrochemical miRNA-21 biosensor

Tawatchai Kangkamano [a, b, c], Apon Numnuam[a, b, c], Warakorn Limbut[a, b, d], Proespichaya Kanatharana[a, b, c], Tirayut Vilaivan[f] and Panote Thavarungkul[a, b, e]*

[a] *Trace Analysis and Biosensor Research Center, Prince of Songkla University, Hat Yai, Songkhla 90112, Thailand*

[b] *Center of Excellence for Innovation in Chemistry, Faculty of Science, Prince of Songkla University, Hat Yai, Songkhla 90112, Thailand*

[c] *Department of Chemistry, Faculty of Science, Prince of Songkla University, Hat Yai, Songkhla 90112, Thailand*

[d] *Department of Applied Science, Faculty of Science, Prince of Songkla University, Hat Yai, Songkhla 90112, Thailand*

[e] *Department of Physics, Faculty of Science, Prince of Songkla University, Hat Yai, Songkhla 90112, Thailand*

[f] *Organic Synthesis Research Unit, Department of Chemistry, Faculty of Science, Chulalongkorn University, Bangkok 10330, Thailand*

* *Corresponding author at: Department of Physics, Faculty of Science, Prince of Songkla University, Hat Yai, Songkhla 90112, Thailand*

Tel.: +66 74 288753; fax: +66 74 558849.

E-mail address: panote.t@psu.ac.th (P. Thavarungkul).

Abstract

A label-free electrochemical miRNA biosensor was developed based on a pyrrolidinyl peptide nucleic acid (acpcPNA)/polypyrrole (PPy)/silver nanofoam (AgNF) modified electrode. The AgNF was electrodeposited as redox indicator on a gold electrode, which was then functionalized with an electropolymerized layer of PPy, a conducting polymer, to immobilize the PNA probes. The fabrication process was investigated by electrochemical impedance spectroscopy. The biosensor was used to detect miRNA-21, a biomarker abnormally expressed in most cancers. The signal was monitored by the change in current of the AgNF redox reaction before and after hybridization using cyclic voltammetry. Two PNA probe lengths were investigated and the longer probe exhibited a better performance. Nucleotide overhangs on the electrode side affected the signal more than overhangs on the solution side due to the greater insulation of the sensing surface. Under optimal conditions, the electrochemical signal was proportional to miRNA-21 concentrations between 0.20 fM and 1.0 nM, with a very low detection limit of 0.20 fM. The biosensor showed a high specificity which could discriminate between complementary, single-, doubled-base mismatched, and non-complementary targets. Three out of the seven tested plasma samples provided detectable concentrations (63±4, 111±4 and 164±7 fM). The sensor also showed good recoveries (81-119%). The results indicated the possibilities of this biosensor for analysis without RNA extraction and/or amplification, making the sensor potentially useful for both the prognosis and diagnosis of cancer in clinical application.

Keywords: *label-free electrochemical sensor; silver nanofoam; polypyrrole; pyrrolidinyl peptide nucleic acid; miRNA-21*

1. Introduction

MicroRNAs (miRNAs), naturally occurring, small, non-coding RNAs of ~19-25 nucleotides in length, are currently receiving much attention as biomarkers due to their effect on the development of cancer (Hamidi-Asl et al., 2013; Huang et al., 2009). Depending on the type of cancer, miRNAs can either be over-expressed or down-expressed compared to the basal level (Hamidi-Asl et al., 2013). Among the miRNAs, miRNA-21 has attracted much attention as a potential biomarker due to its over-expressed level in many types of solid tumors (Lu et al., 2008; Medina and Slack, 2008) and a great deal of effort has been devoted to developing methods for its analysis (Hong et al., 2013; Kilic et al., 2012; Meng et al., 2013). Biosensors with various transduction mechanisms have been considered as potential approaches (Johnson and Mutharasan, 2014; Keshavarz et al., 2015). Among the signal transduction methods, electrochemically based techniques are considered to be one of the most attractive due to their relatively low-cost, high sensitivity, good specificity and the simplicity of their instrumentation (Hamidi-Asl et al., 2013). Electrochemical biosensors for miRNA detection usually involve the measurement of the change in signal from the hybridization event between the short single-stranded nucleotide probe and the target miRNA (Hamidi-Asl et al., 2013; Lautner and Gyurcsányi, 2014). Since miRNAs in blood plasma and serum are typically present at femto to nanomolar levels (Komatsu et al., 2010; Tsujiura et al., 2010), probe selection and signal enhancement are among the factors to be considered. Recently, peptide nucleic acid (PNA) has attracted attention as a probe of choice.

PNA is a DNA mimic in which the natural deoxyribose-phosphate backbone is replaced by a neutral pseudopeptide chain (Nielsen, 2001). Its neutral backbone lessens the electrostatic repulsion between PNA and RNA, subsequently enhanced hybridization efficiency (Zhang et al., 2009). PNAs with structural variations of the backbone have been used as highly specific probes in electrochemical miRNA biosensors (Fan et al., 2007; Jolly

et al., 2016; Zhang et al., 2009). Pyrrolidinyl PNA with a conformationally rigid D-prolyl-2-aminocyclopentanecarboxylic acid (ACPC) backbone (acpcPNA) is an interesting, relatively new PNA system developed by Vilaivan (Suparpprom et al., 2005; Vilaivan and Srisuwannaket, 2006). The excellent chemical and biological stability, high ability to specifically form stable hybrids at low ionic strength, and powerful mismatch discrimination of acpcPNA toward mismatched RNA compared to the other related PNA or other DNA analogues made this newly designed acpcPNA as a promising probe for nucleic acid detection in biosensors (Vilaivan, 2015).

To detect the hybridization between nucleic acid probes and the target miRNAs, either a labeled (Yin et al., 2012) or a label-free (Hou et al., 2015; Li et al., 2016; Rafiee-Pour et al., 2016) method can be employed. Requiring fewer steps than the labeled method, a recently developed procedure in label-free electrochemical biosensors employs redox indicators and detects the difference between the redox peak currents before and after a hybridization event. This peak current difference enables the monitoring of target analytes (Rafiee-Pour et al., 2016; Xia et al., 2013a). Methylene blue (Rafiee-Pour et al., 2016), ferrocene boronic acid (Xia et al., 2013a) and 1-amino-4-anilinoanthraquinone (Azimzadeh et al., 2016) have been successfully employed as redox indicators.

Simplifying the detection even further, we present a novel label-free electrochemical miRNA biosensor that uses a redox indicator of porous silver nanofoam (AgNF), directly deposited onto a gold electrode. AgNF also provided a platform with a large effective surface area. Together with the coated layer of conducting polypyrrole (PPy) that contains a large number of amine groups, immobilization of the acpcPNA probes could effectively be performed. MiRNA-21 is chosen as a model analyte due to its frequent association with many types of cancers (Medina and Slack, 2008). The response measurement is based on the monitoring of the oxidation current of AgNF in a phosphate buffer saline (PBS) using cyclic

voltammetry. The hybridization between the acpcPNA probes and the target miRNA at the electrode surface increases the insulation of the surface and blocks the transfer of electrons which reduces the redox current. The current change generated by such redox reactions before and after hybridization is proportional to the concentration of miRNA-21. The fabrication steps of the developed biosensor were emphasized followed by the investigation of the affecting parameters, i.e., probe length, overhang effect, probe concentration and hybridization time. The performances of the sensor were also assessed, followed by an evaluation of the applicability of the sensor for measuring miRNA-21 in blood plasma samples.

2. Experimental

2.1 Materials

Silver nitrate ($AgNO_3$, 99.9% purity), ammonium chloride (NH_4Cl, 99.8% purity) were from Merck (Darmstadt, Germany). Potassium thiocyanate (KSCN) was from Ajax Finechem (Auckland, New Zealand). Glutaraldehyde (25% solution) was from Fluka (Buchs, Switzerland). Pyrrole monomer and 11-mercapto-1-undecanol (11-MUL) were from Sigma-Aldrich (Steinheim, Germany). All other chemicals used were analytical grade. Diethyl pyrocarbonate (DEPC) treated water was used to prepare the miRNA stock solution. Buffer solutions were used as follows: 10 mM tris(hydroxymethyl)aminomethane-HCl (Tris-HCl, pH 7.80) containing 1.0 mM ethylenediamminetetraacetic acid (EDTA) for DNA stock solution preparation, 10 mM phosphate buffer solution (PB; pH 7.00) for PNA dilution and immobilization and electrode washing, phosphate buffer saline solution (PBS; pH 7.00) containing 0.10 M KCl as the supporting electrolyte for cyclic voltammetric measurement. All sample tubes, microtips and glassware were treated with DEPC to minimize the effect of RNases on the stability of miRNAs and autoclaved to inactivate traces of DEPC.

The 9-mer C-terminal lysine-modified acpcPNA (Ac-TTTTTTTTT-LysNH_2) denoted 'acpcPNA-T9 probe', the 12-mer mixed base lysine-modified acpcPNA (Ac-AGTCTGATAAGC-LysNH_2) denoted 'acpcPNA-12 probe' and the15-mer mixed base C lysine-modified acpcPNA (Ac-TCAGTCTGATAAGCT-LysNH_2) denoted 'acpcPNA-15 probe' were synthesized according to the published protocol (Suparpprom et al., 2005; Vilaivan and Srisuwannaket, 2006) by Mrs. Chotima Vilaivan at Chulalongkorn University, Thailand. The acpcPNA probes were purified by reverse phase HPLC (to > 90% purity) and their identities verified by MALDI-TOF mass spectrometry (acpcPNA-T9: *m*/*z* calcd. 3179.4 found 3179.4; acpcPNA-12: *m*/*z* calcd. 4257.6 found 4257.8; acpcPNA-15: *m*/*z* calcd. 5239.6 found 5245.8).

All the target oligonucleotides used in this study were synthesized and purified through HPLC by Pacific Science Co., Ltd., Thailand. The complementary DNA and miRNA were preliminarily used to study the electrode's fabrication and optimization parameters. All oligonucleotides used in the specificity study were "RNA-mimics", DNA sequences in which thymine bases have been replaced by uracil bases. These sequences are shown as follows: bold italics and underlining indicate mismatched and non-hybridizing segments, respectively. The prefixes r and d indicate RNA and DNA.

For the acpcPNA-T9 probe

Complementary DNA

DNA-A9: 5′-dAAAAAAAAA-3′

For the acpcPNA-12 probe

Complementary DNA

DNA overhang-1: 5′-d<u>TA</u>GCTTATCAGACT<u>GATGTTGA</u>-3′

DNA overhang-2: 5′-d<u>AGTTGTAGA</u>GCTTATCAGACT<u>T</u>-3′

For acpcPNA-15 probe

Complementary miRNA

miRNA-21: 5′-rUAGCUUAUCAGACUGAUGUUGA-3′

miRNA-21 mimics: 5′-dUAGCUUAUCAGACUGAUGUUGA-3′

Single mismatched miRNA

1MT mimics: 5′-dUAGCUUAU***G***AGACUGAUGUUGA-3′

Double mismatched miRNA

2MT mimics: 5′-dUAGCUUA***G***C***G***GACUGAUGUUGA-3′

Non-complementary miRNA

miRNA-122 mimics: 5′-dUGGAGUGUGACAAUGGUGUUUG-3′

miRNA-155 mimics: 5′-dUUAAUGCUAAUCGUGAUAGGGGU-3′

2.2 Apparatus

The electrode modification process was investigated by electrochemical impedance spectroscopy (EIS) in 10 mL 0.30 M PBS, over a frequency range of 10 kHz to 1 mHz with an AC voltage amplitude of 0.010 V versus Ag/AgCl with a Pt wire counter electrode using a μAutolab Type III electrochemical impedance analyzer (Metrohm Autolab B.V., The Netherlands). The impedance spectra were fitted to a Randle's equivalent circuit by the FRA software to obtain the charge transfer resistance (R_{ct}). The fabricated platform was characterized by scanning electron microscopy (SEM) (JSM-5200 LV, JEOL, Japan) and energy dispersive X-ray spectroscopy (EDX). A three-electrode system electrochemical measurements were also performed using a μAutolab Type III controlled by a potentiostat-galvanostat with NOVA 1.8 software.

2.3 Preparation of PPy/AgNF/Au electrode

A gold rod (3.0 mm diameter, 99.99% purity) was polished with successively finer alumina slurries of 5, 1, and 0.3 μm and electrochemically etched in 0.50 M sulfuric acid for 25 cycles (0.10-1.50 V, scan rate 100 mV s^{-1}). Silver was galvanostatically electrodeposited

on the Au surface at room temperature for 20 s, with a controlled current of -0.010 A from a 10 mL aqueous electrolyte consisting of 0.020 M $AgNO_3$, 1.5 M KSCN and 2.0 M NH_4Cl in a batch cell. The obtained porous AgNF/Au electrode was washed with deionized water and dried with nitrogen gas. PPy was electropolymerized onto the AgNF/Au electrode by 3 cycles of cyclic voltammetry between 0.40 and 0.90 V at 20 mV s^{-1} in a solution containing 0.10 M $LiClO_4$ and 0.20 M pyrrole monomer, then rinsed with deionized water.

2.4 PNA probes immobilization

The fabrication procedure of the biosensor is shown in Fig.1. The PPy/AgNF/Au electrode was immersed in 5.0% v/v glutaraldehyde (GA) for 30 min to activate the PPy surface with aldehyde groups. After rinsing with deionized water, 20.0 μL of 5.0 μM acpcPNA probes was placed on top and kept overnight at 4°C. The electrode was rinsed with 10 mM PB to remove unbound probes and treated with 1.0 M ethanolamine pH 8.00 for 10 min to deactivate all the remaining aldehyde groups not coupled to the immobilized acpcPNA probe. Finally, the modified electrode was immersed in 1.0 mM of 11-MUL for 1 h at room temperature to block the remaining bare spots on the electrode, thus preventing non-specific binding (Thipmanee et al., 2012). While not in use the electrode was kept in 10 mM PB at 4°C.

Fig.1 here

2.5 Probe hybridization and electrochemical measurements

A 10.0 μL of target miRNA was drop casted onto the PNA immobilized electrode and allowed for a hybridization time of 15 min (before optimization) at room temperature. The electrode was then rinsed with 10 mM PB before immersion in a batch cell containing 10 mL of 10 mM PBS. An equilibration time of 5 min was allowed before measuring by cyclic voltammetry (CV) using a step potential of 2.50 mV; a scan rate of 100 mV s^{-1}; an interval

time of 0.025 s and a scan potential between -0.40 and 0.60 V. The hybridization between the PNA probes and the target miRNA increases the insulation at the electrode surface and blocks the interfacial charge transfer between the electrode and electrolyte that reduces the redox current of the AgNF (Fig.1). The reduction in the oxidation peak current (ΔI) was taken as the response. Next, 10.0 μL of the regeneration solution (50 mM NaOH) was dropped onto the electrode surface and left for 3 min to dissociate the probe-target hybrid. After rinsing with deionized water and the oxidation peak returned to its original height, a new analytical cycle is performed.

2.6 Specificity study

The specificity was evaluated by comparing the signal of the complementary miRNA-21 to the single-base and double-base mismatched targets (homology factors 95.5% and 90.9%, respectively). We also studied the signals of miRNA-122 and miRNA-155 since they have higher homology factors (54.5% and 40.9%) to miRNA-21 than other miRNAs and could therefore produce a false positive result. The % signal suppression (%SS) (Eq.1) was used to assess the ability of the developed sensor to discriminate between interferences and target. A higher %SS indicates a better specificity.

$$\%SS = \frac{\Delta I_{\text{complementary oligonucleotides}} - \Delta I_{\text{mismatched oligonucleotides}}}{\Delta I_{\text{complementary oligonucleotides}}} \times 100 \qquad (1)$$

3. Results and discussion

3.1 Surface morphology of the modified electrode

Hydrogen bubbles were used as templates for the plating of porous silver nanofoam onto the gold electrode (AgNF/Au). They were generated by applying a high cathodic current in an aqueous containing $AgNO_3$ as the Ag^+ source, NH_4Cl as a H_3O^+ producer to accelerate

hydrogen evolution, and KSCN as a complexing ligand to prevent the precipitation of Ag^+ (Cherevko et al., 2010). By applying a cathodic current, silver ions were reduced within the bubble templates and left behind a porous foam-like structure of silver (Ag^0). This AgNF has porous walls with a particle-like structure in the nanoscale range (Fig.2A). The electrochemically polymerized PPy showed as a smooth thin film covering the AgNF layer (Fig.2B). This layer of amine rich-conducting PPy would enable a large amount of PNA probes to be immobilized. The EDX spectrum of the electrode surface also confirmed the presence of PPy and AgNF with a good distribution of C and N (from PPy) and Ag (from AgNF) that can be observed through the X-ray mapping (Supplementary data Fig.S1).

Fig.2 here

3.2 Electrochemical characterizations

The stepwise modification of the PNA biosensor was studied by EIS. The charge transfer resistance (R_{ct}), presented as the semicircle diameter of a Nyquist plot in the high-frequency region, was obtained by fitting the data to a suitable equivalent circuit (inset, Figs.2C-D). A bare gold electrode demonstrated a small semicircle impedance spectrum and a linear part (Fig.2C) indicating a diffusion limiting process in the lower frequency region. The low R_{ct} of 136±2 kΩ indicated a small charge transfer resistance. After the electrodeposition of AgNF (Fig.2D), the electrode presented a much larger semicircle with an R_{ct} of 401±1 kΩ. The surprisingly large impedance was likely caused by the porous nature of the AgNF. The small pores on the surface may lead to the formation of the double electrical layer (at the same concentration of electrolyte) on each side of the porous wall that are very close to each other and start to affect ion movement inside the nanopores causing high impedance in the system (Kant et al., 2014). When the conducting PPy was deposited (PPy/AgNF/Au), a much smaller semicircle with an R_{ct} of 57±3 kΩ was obtained due to the

good conductivity of PPy and the better ion movement inside the shallower pores that were a result of the covering polymer. Without the porous AgNF, the R_{ct} of PPy on the bare gold surface (PPy/Au) was much lower (47±3 kΩ). Although the resistance was lower, the surface area would be less and allowed a lesser amount of immobilized PNA probes. When the cross-linker glutaraldehyde (GA) was applied (GA/PPy/AgNF/Au), the R_{ct} increased to 116±4 kΩ due to the insulating nature of GA. R_{ct} slightly increased again (163±8 kΩ) when acpcPNA probes (acpcPNA-T9) were immobilized (PNA/GA/PPy/AgNF/Au) on the electrode. When 11-MUL was added (MUL/PNA/GA/PPy/AgNF/Au), the R_{ct} increased further (332±4 kΩ) due to the blocking of interfacial charge transfer caused by its insulating nature. Finally, when 1.0×10^{-5} M of a DNA (A9) with a complementary sequence to the acpcPNA-T9 probe was tested (DNA/MUL/PNA/GA/PPy/AgNF/Au), the hybridization caused the R_{ct} to increase significantly to 466±5 kΩ due to further charge blocking by the DNA bound to the PNA probe on the electrode surface. The sequential changes of R_{ct} during the modification steps demonstrated that a sensing interface was effectively constructed and that the biosensor was successfully fabricated.

3.3 Optimization of parameters

3.3.1 The effect of PNA probe lengths and overhang

To obtain a good binding efficiency, 12 bases and 15 bases probes, acpcPNA-12 and acpcPNA-15, were investigated in comparison. In this preliminary test, target DNA with the same 22 bases as the miRNA-21 was used due to its lower cost and better stability than miRNA. Fig.3A shows the expected base pairing between the two acpcPNA probes and the DNA targets. DNA overhang-1 has the same binding position as the miRNA-21 with the longer overhang on the solution side while the longer overhang of DNA overhang-2 is on the electrode side.

The plots between the response (ΔI) of the DNA overhang-1 between 1.0×10^{-16} and 1.0×10^{-4} M showed two linear ranges for both probes. The first linear range of the 12 bases probe was 1.0×10^{-13} - 5.0×10^{-8} M and the second with a higher sensitivity (slope) at 5.0×10^{-8} - 1.0×10^{-5} M (Supplementary data Fig.S2). The LOD, expressed by the concentration of the analyte at which the extrapolated linear portion of the calibration curve intercepted with the final lowest concentration level segment of the calibration plot (Buck and Lindner, 1994), was 1.0×10^{-13} M. For the 15 bases probe, better performance was obtained with a slightly wider first linear range of 1.0×10^{-14} to 1.0×10^{-7} M, with the second at 1.0×10^{-7} - 1.0×10^{-5} M. The LOD, 1.0×10^{-14} M, was also better. The existence of two slopes is similar to the result reported by an earlier work (Li et al., 2014). This may be because there is a small amount of target DNA in the solution at low concentration creating a few PNA-DNA hybrids, hence the slightly increase of the ΔI. When the DNA concentration was sufficiently high, the DNAs and probes that were already paired might be able to induce a change of the unpaired probe orientation to provide a better accessibility to DNAs. Thus, the hybridization was more efficiency leading to a larger change of current. However, for further experiments, since miRNA-21 is typically found in plasma samples at very low concentrations (~10 fM - 0.9 nM) (Komatsu et al., 2010; Tsujiura et al., 2010), the lower concentration range was being focused.

Fig.3B shows the effect of the different overhangs for both the acpcPNA-12 and acpcPNA-15 probes. Sensitivities of the target DNA overhang-2 are expressed by the slope of calibration plot between ΔI and the logarithm of the concentrations of target. When the overhang was directed towards the electrode side, the sensitivities were higher than they were when the overhang pointed to the solution side (DNA overhang-1). This is most likely because the longer the overhang length on the electrode surface, the more insulated the electrode surface becomes, producing a larger redox current change from the AgNF. This was

confirmed by the impedance spectra which presented higher R_{ct} of 237±4 kΩ and 388±8 kΩ compared to 221±7 kΩ and 327±8 kΩ for acpcPNA-12 and acpcPNA-15 hybridized with DNA overhang-2 and DNA overhang-1, respectively. Thus, when detecting a change in current, as in this work, this behavior is useful and may be used in future designs of the probe so that the target overhang would be directed towards the electrode surface to enhance the response and sensitivity of the developed sensor.

3.3.2 PNA probe concentration and hybridization time

The amount of accessible immobilized probe on the electrode surface is considered a major factor affecting the efficiency of hybridization (Keighley et al., 2008). The amount of the acpcPNA-15 probes used for the immobilization was investigated with miRNA-21 as the target. Before the optimization, the hybridization efficiencies of the PNA-DNA (Section 3.3.1) and PNA-miRNA-21 hybrids were compared. There were no significant differences between the sensitivities (P>0.05) of the two target types (Supplementary data Fig.S3). These results suggest that although acpcPNA binds more strongly to DNA (Vilaivan, 2015), it can also be useful as an RNA probe.

Fig.3 here

To find the most suitable PNA probe concentration, different concentrations of acpcPNA-15 (20 μL of 5.0, 10.0 and 15.0 μM) were immobilized on PPy/AgNF modified electrode. The responses of miRNA-21 with 15 min of hybridization time are shown in Fig.4A. As expected, both the sensitivities (slope in Fig.4A) and LODs were better at higher concentrations. The LODs were 20 fM, 0.030 fM and 0.010 fM for 5.0, 10.0 and 15.0 μM of PNA, respectively. This is likely because the increased amount of PNA probes resulted in more available binding sites for the targets to produce more PNA-miRNA hybrids, which increased the insulating property of the electrode surface and therefore the change in the

measured current. However, the highest concentration (15.0 μM) provided a shorter range of linearity. This is because more immobilized probes made the surface more insulated and provided a much lower original current before the hybridization (Fig.4A-inset). Thus, there was a smaller gap between the response without analyte and the maximum signal of analyte detection in the saturated condition. Therefore, the sensor that could provide a good LOD and good linearity was 10.0 μM of PNA probe, and this was selected to measure miRNA-21.

The aim of the work to develop a sensor that can diagnose within a short analysis time, and so we tested the sensor at a reduced hybridization time of 5 min with the acpcPNA-15 probe, immobilized at 10.0 μM with a target miRNA-21. Hybridization time of 5 min gave a slightly lower sensitivity and higher LOD (0.20 fM c.f. 0.030 fM for 15 min) (Fig.4B) than were recorded at 15 min. However, this is more than sufficient for miRNA-21 detection in real plasma samples which are normally found around 10 fM - 0.9 nM (Komatsu et al., 2010; Tsujiura et al., 2010). Therefore, a hybridization time of 5 min was used for further target miRNA detection. From the presented results, this developed sensor has the advantage of measuring miRNA-21 in a short time. Moreover, if the sample has a very low concentration of analyte, the hybridization time could be increased accordingly and at 15 min hybridization time, a target concentration as low as 0.030 fM could be readily measured.

Fig.4 here

3.4 Analytical performances

3.4.1 Linearity, LOD

Fig.4B shows the relationship between current change and the logarithm of the concentrations of target miRNA-21 under the optimal conditions and 5 min of hybridization, together with an example of the measured current signal for different concentrations of the target (Fig.4B-inset). The linear range was between 2.0×10^{-16} M and 1.0×10^{-9} M with the

regression equation of ΔI = (1.87±0.05) log [miRNA-21] + (33±1) and a relatively low LOD of 0.20 fM. This LOD value is more than sufficient for measuring normal and abnormal miRNA-21 found in real plasma samples. The obtained results indicated that the newly designed acpcPNA provided a strong binding affinity and excellent sequence specificity towards miRNA that complemented both the PPy covering on the porous structure of AgNF, which effectively immobilized the probe, and the AgNF redox indicator.

3.4.2 Specificity

In this specificity study, we used a miRNA-21 mimic after its responses were proven not significantly different from that of standard miRNA-21 (P>0.05 two-way ANOVA) (Supplementary data Fig.S4). The results indicated that the acpcPNA can specifically bind not only with DNA and RNA but also with RNA mimic. Thus, as an alternative stable standard, this RNA mimic might be useful for future testing in the fabrication of acpcPNA based RNA biosensors. To verify the selectivity of the developed sensor, the probe was hybridized with non-complementary oligonucleotides and tested. A much higher current change was detected from the miRNA-21 and miRNA-21 mimic than from the single base (1MT), double bases (2MT) mismatched target and miRNA-122 and miRNA-155 (Fig.5). The %SS of the double mismatched target (88.8-94.4%) were slightly higher than for the single mismatched target (88.3-92.5%). MiRNA-122 and miRNA-155 gave the higher %SS (88.9-95.0% and 90.4-98.9%, respectively) than the single base and double bases mismatched target. The comparison showed the developed sensor's good specificity and its ability to differentiate between the target and other possible interference oligonucleotides.

Fig.5 here

3.4.3 Repeatability and Reproducibility

Six measurements for each of three concentrations of miRNA-21 were performed at 1.0×10^{-15}, 1.0×10^{-13} and 1.0×10^{-11} M (Supplementary Data Fig.6A): the measurements produced RSDs of 9.4%, 4.2% and 5.0%, respectively. We tested the reproducibility of three electrodes, independently fabricated on different days under the same conditions, by measuring a series of 5 miRNA-21 concentrations between 1.0×10^{-15} and 1.0×10^{-11} M. The sensitivities of the three electrodes were 2.07±0.17, 2.03±0.32 and 2.00±0.04 -μA $(\log M)^{-1}$ (Supplementary Data Fig.S6B-C). The relative standard deviation of the average sensitivity was calculated to be 2.0% indicating that the proposed PNA biosensor has acceptable reproducibility.

3.4.4 Reusability

The reusability of the modified electrode was examined by repeatedly analyzing 1.0×10^{-7} M of miRNA-21. After each analysis, 10.0 μL of 50 mM NaOH was dropped onto the miRNA-21 hybridized electrode to break the PNA-RNA hybrids. The Ag oxidation peak current change (ΔI) of the first response was taken as 100%. The current changes of the subsequent analysis cycles were compared to the first one. It was found that the hybridization procedure could be repetitively performed for thirty cycles with an average of 97±3% (3.1% RSD) before the response was decreased to be less than 90% (Supplementary data Fig.S5A). The obtained result indicated that the proposed PNA biosensor has a satisfactory reusability. The decrease in the relative response was likely due to the loss of some parts of the modified layers on the electrode, especially AgNF, which was indicated by the reduced silver redox peaks observed after scanning the used electrode in PBS (Supplementary data Fig.S5B).

The analytical properties of the sensor toward miRNA-21 detection were compared with those of other electrochemical biosensors as listed in Table 1. Using the shortest incubation time of 5 min, the developed PNA biosensor provided a satisfactory linear range

that was wider than most reported biosensors. The width of the linear range may be attributed to the neutral backbone of the acpcPNA which reduced the electrostatic repulsion between the two hybridized strands, increasing their affinity for each other. Moreover, the sensor exhibited a relatively low limit of detection (0.20 fM) that was better than the LODs in most cited reports. By increasing the hybridization time (15 min), the developed sensor could measure at a lower concentration range, down to 0.030 fM. The lower detection limit is most likely due to a good synergy between the excellent binding property of the acpcPNA probe toward miRNA-21 and the large surface area of the amine-rich PPy covering the porous structure of AgNF that facilitated probe immobilization. In addition, a good conductive property of the AgNF layer as a redox indicator directly deposited onto the electrode (not in solution) also took a part in helping to increase the sensitivity of this sensor. Although the obtained LODs were slightly higher than those reported in some other works (Liu et al., 2017; Shuai et al., 2017), they were more than sufficient for measuring miRNA-21 found in real plasma samples (10 fM - 0.9 nM). Moreover, the design of the present label-free biosensor is simple and obviated the need for labeling molecules, thus reducing the cost and operational complexity of the assay. With these advantages, the developed label-free electrochemical acpcPNA biosensor would be potentially useful as an alternative tool for the detection of miRNA-21 or other miRNAs both for screening tests and diagnostics of cancer in clinical applications.

3.5 The concentration of miRNA-21 in human plasma samples

To demonstrate the applicability of the acpcPNA biosensor for analyzing circulating miRNAs, human plasma samples collected from Songklanagarind Hospital, Hat Yai, Thailand were tested. The study of matrix effect was carried out by comparing the calibration plot obtained from standard miRNA-21 solution and spiked sample solutions at 0, 10, 50, and 100 times dilution and analyzed under optimal conditions. Spiked samples without and with a

dilution factor of 10 and 50 times provided very small signal peaks, much lower than the signal of the highest concentration of analyte in buffer. This was likely because non-specific adsorption of molecules in the real sample onto the electrode surface obstructed the electron transfer between the electrolyte and the AgNF. This effect was negligible at the 100 times dilution in which the slope of the spiked samples showed no significant difference to that of standard miRNA-21 (P>0.05 two-way ANOVA). Thus, there was no matrix effect at this dilution and human plasma samples could be analyzed after diluting 100 times. The responses obtained from the samples were used to calculate their concentrations from the standard calibration equation and then multiplied by the dilution factor of 100. Seven samples were tested: miRNA-21 could be detected in three samples at 63±4, 111±4 and 164±7 fM, while miRNA-21 were not detectable in the other four samples (<20 fM).

To validate the acpcPNA biosensor, a recovery experiment was conducted by adding 20, 50, 70, 100 and 150 fM of miRNA-21 into three human plasma samples to obtain final concentrations of 0.2, 0.5, 0.7, 1.0 and 1.5 fM after 100 times dilution. These spiked samples were then analyzed by the developed sensor. Recoveries of the five miRNA-21 concentrations from the three plasma samples were in the range of 81-119% (Supplementary data Table S1), which are within the acceptable range of 40-120% (Taverniers et al., 2004). The relative standard deviations (RSDs) were all below 14 %. These are well within the acceptance limit, which is <30% for 1 ppb of analyte (Taverniers et al., 2004) (for miRNA-21 with a molecular weight of 6,652 g/mol (Kilic et al., 2012) this was equal to 1.50×10^{-10} M or 0.15 fM). In addition, a plot between the measured and the spiked concentrations of miRNA-21 in a plasma sample (Supplementary data Fig.S7) showed good correlation with a slope of 0.9803 and r = 0.9783. These results demonstrated the potential of the developed biosensor for the direct detection of miRNA-21 in complex biological samples, making it a very good candidate for future clinical application. A point that should be mentioned here is that

circulating miRNAs in plasma samples have many forms, free miRNA, encapsulated in vesicles and bound to proteins (Cheng, 2015) and this may affect the response (Metcalf et al., 2016). Further investigation of the effect of these various forms would be useful.

4. Conclusions

A label-free electrochemical biosensor using the newly designed pyrrolidinyl peptide nucleic acid (acpcPNA) probes immobilized on a PPy/AgNF modified Au electrode was successfully developed for the cyclic voltammetric detection of cancer-associated miRNA-21. The porous structure of AgNF, covered by an amine-rich conducting polymer of PPy, was used as a stationary redox indicator that acted both as a sensing element for measuring the hybridization event and a platform to provide a large effective surface area for immobilizing the PNA probes. The immobilization of the probe by this platform was combined with the strong binding affinity and excellent sequence specificity towards miRNA-21 of acpcPNA. Without using any label molecules, complex procedure or expensive apparatus, the sensor permitted a potential detection of miRNA-21 within a short analysis time (5 min) together with a relatively low LOD of 0.20 fM. This sensor could be applied to directly detect miRNA-21 in a complex biological sample by easily diluting the samples, without the need of prior extraction and purification of the miRNAs. In addition, this PNA biosensor also exhibited an excellent selectivity which could discriminate between miRNA-21 from other possible interfering oligonucleotides. With all these advantages, this developed biosensor would be a potential alternative tool for the detection of miRNA-21 in clinical diagnosis and prognosis. Its application in array sensors for detecting multiple targets is also a possibility.

Acknowledgements

This work was supported by the Thailand Research Fund (TRF) grant no. DPG 5780002. We would also like to thank the Center of Excellence for Innovation in Chemistry (PERCH-CIC), Trace Analysis and Biosensor Research Center (TAB-RC) at Prince of Songkla University of Thailand. The financial support for Tawatchai Kangkamano from The National Science and Technology Development Agency (NSTDA), Ministry of Science and Technology of Thailand and Thaksin University of Thailand are also gratefully acknowledged. Thanks also to Mr Thomas Duncan Coyn, Faculty of Science, Prince of Songkla University, Hat Yai, Songkhla, Thailand for assistance with the English.

References

Azimzadeh, M., Rahaie, M., Nasirizadeh, N., Ashtari, K., Naderi-Manesh, H., 2016. Biosens. Bioelectron. 77, 99-106.

Buck, R.P., Lindner, E., 1994. Pure & App. Chem. 66(12), 2527-2536.

Cheng, G., 2015. Adv. Drug Deliv. Rev. 81, 75-93.

Cherevko, S., Xing, X., Chung, C.-H., 2010. Electrochem. Commun. 12(3), 467-470.

Fan, Y., Chen, X., Trigg, A.D., Tung, C.-h., Kong, J., Gao, Z., 2007. J. Am. Chem. Soc. 129(17), 5437-5443.

Hamidi-Asl, E., Palchetti, I., Hasheminejad, E., Mascini, M., 2013. Talanta. 115, 74-83.

Hong, C.-Y., Chen, X., Liu, T., Li, J., Yang, H.-H., Chen, J.-H., Chen, G.-N., 2013. Biosens. Bioelectron. 50, 132-136.

Hou, T., Li, W., Liu, X., Li, F., 2015. Anal. Chem. 87(22), 11368-11374.

Huang, Z., Huang, D., Ni, S., Peng, Z., Sheng, W., Du, X., 2009. Int. J. Cancer. 127, 118-126.

Johnson, B.N., Mutharasan, R., 2014. Analyst. 139(7), 1576-1588.

Jolly, P., Batistuti, M.R., Miodek, A., Zhurauski, P., Mulato, M., Lindsay, M.A., Estrela, P., 2016. Sci. Rep. 6, 36719.

Kant, K., Priest, C., Shapter, J.G., Losic, D., 2014. Sensors. 14(11), 21316-21328.

Keighley, S.D., Estrela, P., Li, P., Migliorato, P., 2008. Biosens. Bioelectron. 24(4), 906-911.

Keshavarz, M., Behpour, M., Rafiee-pour, H.-A., 2015. RSC Adv. 5(45), 35651-35660.

Kilic, T., Topkaya, S.N., Ozkan Ariksoysal, D., Ozsoz, M., Ballar, P., Erac, Y., Gozen, O., 2012. Biosens. Bioelectron. 38(1), 195-201.

Komatsu, S., Ichikawa, D., Takeshita, H., Tsujiura, M., Morimura, R., Nagata, H., Kosuga, T., Iitaka, D., Konishi, H., Shiozaki, A., Fujiwara, H., Okamoto, K., Otsuji, E., 2010. Br. J. Cancer. 105(1), 104-111.

Lautner, G., Gyurcsányi, R.E., 2014. Electroanalysis. 26(6), 1224-1235.

Li, F., Peng, J., Wang, J., Tang, H., Tan, L., Xie, Q., Yao, S., 2014. Biosens. Bioelectron. 54, 158-164.

Li, W., Hou, T., Wu, M., Li, F., 2016. Talanta. 148, 116-121.

Liu, L., Chang, Y., Xia, N., Peng, P., Zhang, L., Jiang, M., Zhang, J., Liu, L., 2017. Biosens. Bioelectron. 94, 235-242.

Liu, L., Xia, N., Liu, H., Kang, X., Liu, X., Xue, C., He, X., 2014. Biosens. Bioelectron. 53, 399-405.

Lu, Z., Liu, M., Stribinskis, V., Klinge, C.M., Ramos, K.S., Colburn, N.H., Li, Y., 2008. Oncogene. 27, 4373-4379.

Mandli, J., Mohammadi, H., Amine, A., 2017. Bioelectrochemistry. 116, 17-23.

Medina, P.P., Slack, F.J., 2008. Cell Cycle. 7(16), 2485-2492.

Meng, X., Zhou, Y., Liang, Q., Qu, X., Yang, Q., Yin, H., Ai, S., 2013. Analyst. 138(12), 3409-3415.

Metcalf, G.A.D., Shibakawa, A., Patel, H., Sita-Lumsden, A., Zivi, A., Rama, N., Bevan, C.L., Ladame, S., 2016. Anal. Chem. 88 (16), 8091-8098.

Nielsen, P.E., 2001. Curr. Opin. Biotechnol. 12(1), 16-20.

Rafiee-Pour, H.-A., Behpour, M., Keshavarz, M., 2016. Biosens. Bioelectron. 77, 202-207.

Shuai, H.-L., Huang, K.-J., Zhang, W.-J., Cao, X., Jia, M.-P., 2017. Sens. Actuators, B. 243, 403-411.

Su, S., Cao, W., Liu, W., Lu, Z., Zhu, D., Chao, J., Weng, L., Wang, L., Fan, C., Wang, L., 2017. Biosens. Bioelectron. 94, 552-559.

Suparpprom, C., Srisuwannaket, C., Sangvanich, P., Vilaivan, T., 2005. Tetrahedron Lett. 46(16), 2833-2837.

Taverniers, I., De Loose, M., Van Bockstaele, E., 2004. Trends Anal. Chem. 23(8), 535-552.

Thipmanee, O., Samanman, S., Sankoh, S., Numnuam, A., Limbut, W., Kanatharana, P., Vilaivan, T., Thavarungkul, P., 2012. Biosens. Bioelectron. 38(1), 430-435.

Tsujiura, M., Ichikawa, D., Komatsu, S., Shiozaki, A., Takeshita, H., Kosuga, T., Konishi, H., Morimura, R., Deguchi, K., Fujiwara, H., Okamoto, K., Otsuji, E., 2010. Br. J. Cancer. 102(7), 1174-1179.

Vilaivan, T., 2015. Acc. Chem. Res. 48(6), 1645-1656.

Vilaivan, T., Srisuwannaket, C., 2006. Org. Lett. 8(9), 1897-1900.

Xia, N., Wang, X., Deng, D., Wang, G., Zhai, H., Li, S.-J., 2013a. Int. J. Electrochem. Sci. 8, 9714-9722

Xia, N., Zhang, L., Wang, G., Feng, Q., Liu, L., 2013b. Biosens. Bioelectron. 47, 461-466.

Xia, N., Zhang, Y., Wei, X., Huang, Y., Liu, L., 2015. Anal. Chim. Acta. 878, 95-101.

Yin, H., Zhou, Y., Zhang, H., Meng, X., Ai, S., 2012. Biosens. Bioelectron. 33(1), 247-253.

Zhang, G.-J., Chua, J.H., Chee, R.-E., Agarwal, A., Wong, S.M., 2009. Biosens. Bioelectron. 24(8), 2504-2508.

Zhou, Y., Zhang, Z., Xu, Z., Yin, H., Ai, S., 2012. New J. Chem. 36(10), 1985-1991.

Figure legends

Fig.1 The fabrication procedure and detection principle of the developed label-free biosensor

Fig.2 SEM images of modified electrodes; (A) AgNF layer and (B) PPy covered AgNF layer and EIS spectra of Nyquist plots of the shown equivalent circuit of different modified electrode surfaces; (C) bare Au electrode and (D) the different layers of electrode modification. Supporting electrolyte, 0.30 M PBS solution pH 7.00 containing 0.10 M KCl. The frequency range was between 10 kHz -1 mHz.

Fig.3 (A) The expected patterns of the hybridization between the acpcPNA-12 and acpcPNA-15 probes and DNA overhang-1 with the overhanging part in the solution and DNA overhang-2 with the overhanging part on the electrode surface. (B) The calibration curves obtained from measuring the 22 bases DNA.

Fig.4 (A) The current changes of silver oxidation peak current after the hybridization of different concentrations of acpcPNA-15 probe (20 μL of 5.0, 10.0 and 15.0 μM) with different concentrations of miRNA-21. (inset: the CV responses for original signal without miRNA-21, 1.0×10^{-16} M and 1.0×10^{-13} M of miRNA-21) (B) The calibration plots using 10.0 μM of acpcPNA-15 probe immobilized electrode to measure different concentrations of miRNA-21 with 5 and 15 min hybridization times. (inset: the example of the CV responses for miRNA-21 in the concentrations between 1.0×10^{-15} and 1.0×10^{-11} M obtained from using the acpcPNA-15 probe immobilized electrode with 5 min of hybridization time.) The indicated error bars represent the standard deviation of three replications.

Fig.5 The responses of the acpcPNA-15 probes immobilized PPy/AgNF/Au electrode toward different concentrations (1.0 fM, 0.10 pM, 0.010 nM) of miRNA-21, miRNA-21mimics and the four oligonucleotide interferences detection (the single base mismatched target (1MT), the double bases mismatched target (2MT), miRNA-122 and miRNA-155).

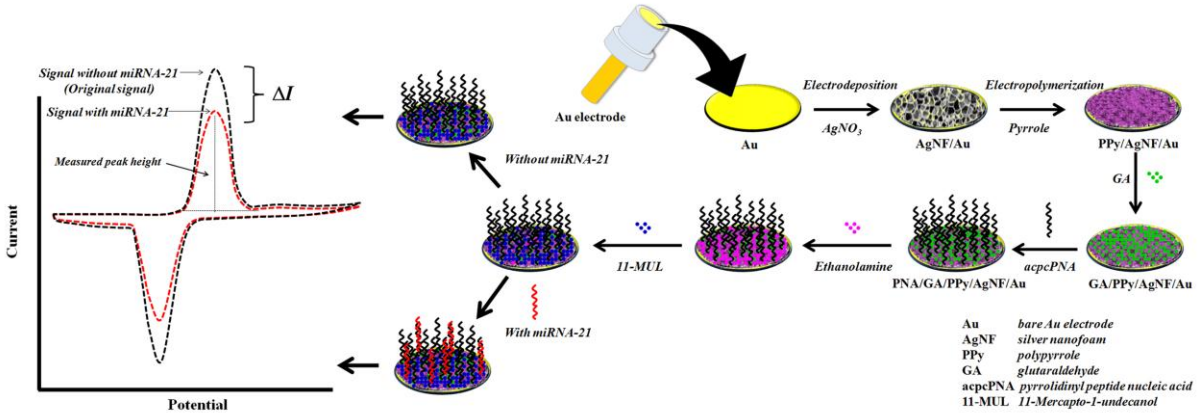

Fig. 1

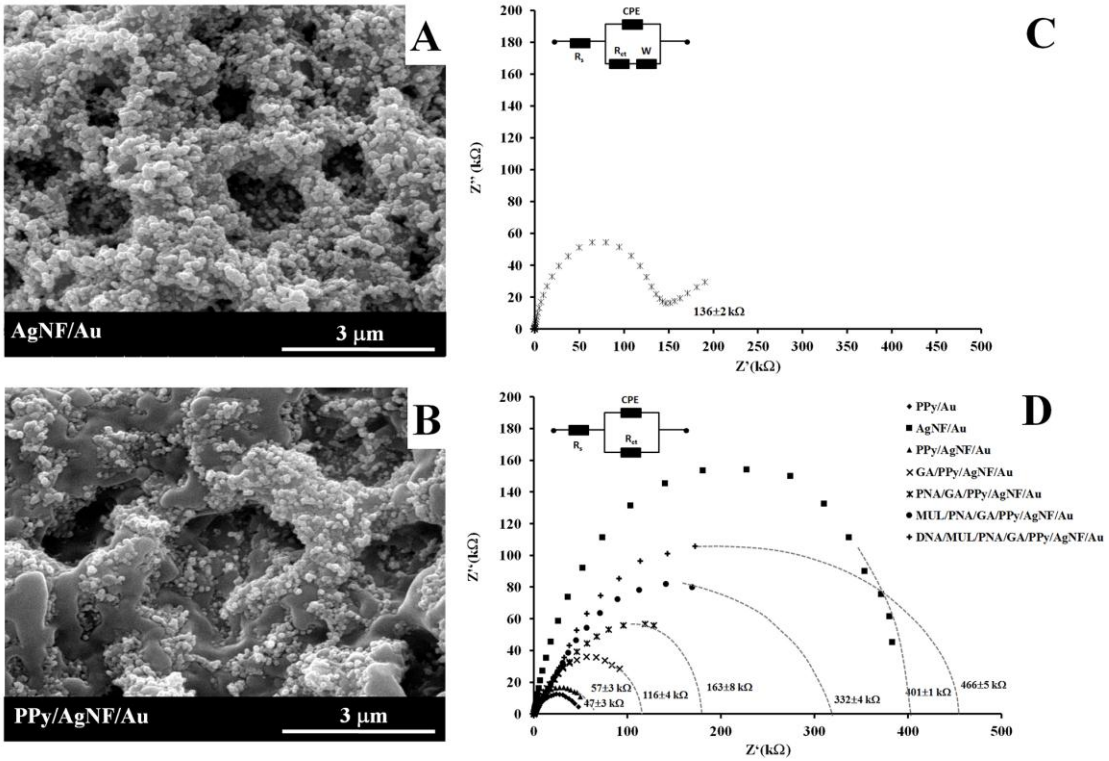

Fig. 2

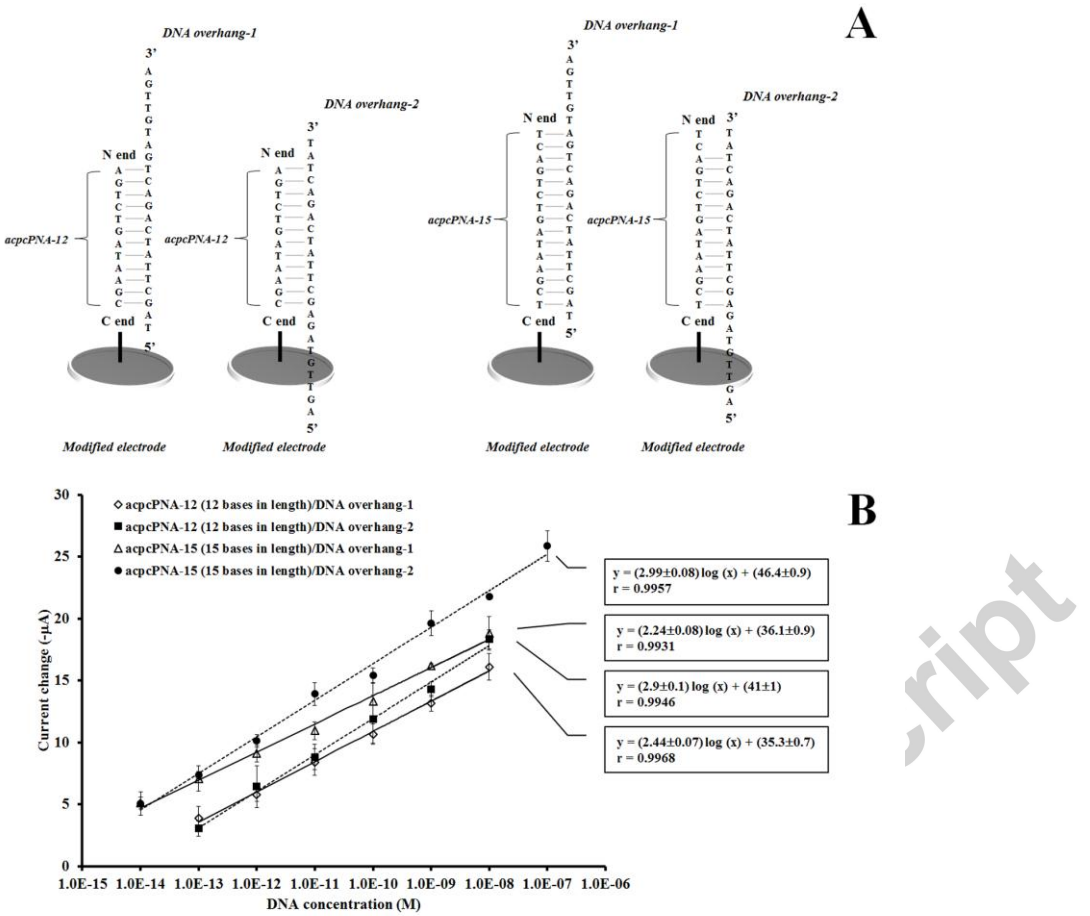

Fig. 3

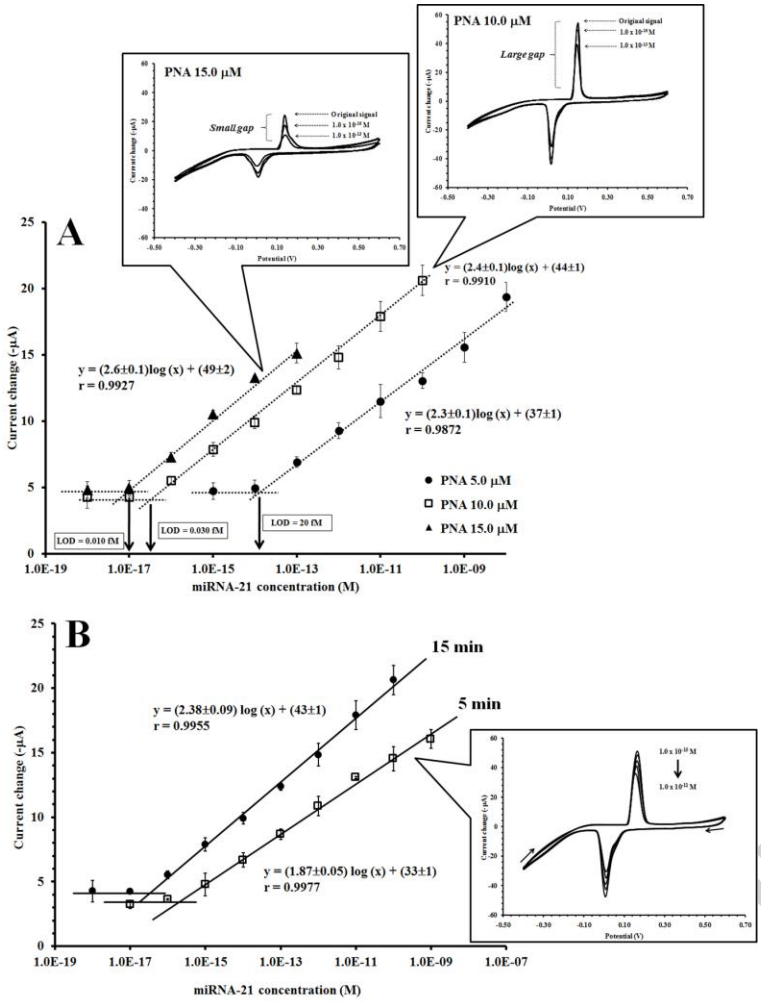

Fig. 4

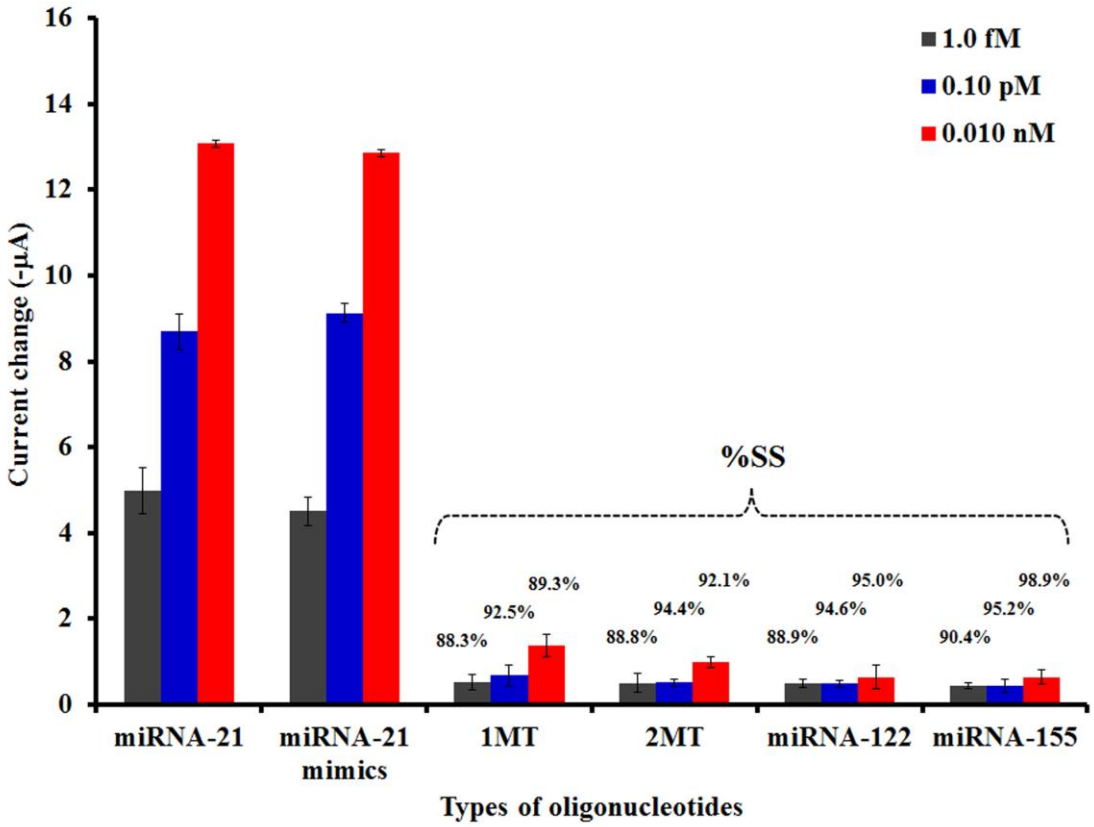

Fig. 5

Table 1

The performance of the fabricated label-free electrochemical acpcPNA based biosensor and other reported biosensors for miRNA-21 detection.

Modification types		Method		Recognition element (probe)	Signaling element	Linearity	LOD	
Label-free electrochemical biosensors								
acpcPNA/PPy/AgNF/AuE		CV		acpcPNA	AgNF	0.2 fM – 1.0		
nM		0.2 fM		5	This work			
						0.03 fM –		
0.1nM	0.03 fM	15						
AgNPs/MPBA/DNA-Au/CGE		LSV		DNA	AgNPs	0.1 fM – 2.0		
pM		0.02 fM	60		(Liu et al., 2017)			
DNA2/DNA1/AuNPs-MoS_2/GCE		EIS		DNA	$[Fe(CN)_6]^{3-/4-}$	10.0 fM – 1.0		
nM		0.45 fM	NR		(Su et al., 2017)			
		DPV		DNA	$[Ru(NH_3)_6]^{3+}$	10.0 fM – 1.0		
nM	0.78 fM	NR						
DNA/MWCNTs/GCE		DPV		DNA	MB	0.1 pM – 0.5 nM	84 fM	

SA-ALP/APBA-biotin-AuNPs/ DNA/AuE	Amp	DNA	p-APP	10.0 fM – 5.0	
pM	3.0 fM	30		(Liu et al.,	
2014)					
DA-AuNPs/ MPBA-AuNPs/ DNA/AuE	DPV	DNA	DA	0.1 pM – 10	
Pm	45 fM	30	(Xia et al., 2013b)		
Labeled electrochemical biosensors					
SA-ALP/biotin-P2/SH-P1/ AuNPs/PGE	DPV	DNA	α-NAP	200 pM – 388	
nM	100 pM	35	(Mandli et al., 2017)		
SA-ALP/DNA-GO-AuNPs/CP/AuNPs/	DPV	DNA	AAP/FcM	0.1fM – 100	
fM	0.05 fM	60	(Shuai et al., 2017)		
MgO/GCE					
SA-ALP/biotin-DNA/AuE	DPV	DNA	AAP/FcM	0.5 fM – 1 pM	0.2 fM
SA-HRP/LNA hairpin /AuNPs/ Gr/AuE	Amp	LNA/DNA	BZ	1.0 pM – 5.0	
nM	0.4 pM	60	(Zhou et al., 2012)		
SA-HRP/biotin-DNA-AuNPs-LNA/	DPV	LNA/DNA	BZ	0.1 pM – 70	
pM	70 fM	150	(Yin et al., 2012)		
DNA-MB/DenAu/Gr/GCE					

acpcPNA, peptide nucleic acid derived from a D-prolyl-2-aminocyclopentanecarboxylic acid backbone; PPy, polypyrrole; AgNF, silver nanofoam; AuE, gold electrode; CV, cyclic voltammetry; AgNPs, silver nanoparticles; MPBA, 4-mercaptophenylboronic acid; CGE, carbon glass electrode; LSV, linear sweep voltammetry; Amp, amperometry; DPV, differential pulse voltammetry; EIS, electrochemical impedance spectroscopy; BZ, benzoquinone; GCE, glassy carbon electrode; Gr, graphene; SA-HRP, streptavidin labeled horseradish peroxidase; NR, not reported; SA-ALP, streptavidin-alkaline phosphatase; biotin-P2, biotin labeled DNA probe 2; SH-P1, thiol terminated capture DNA probe 1; PGE, pencil graphite electrode; α-NAP, α-Naphtol; DA, dopamine; CP, DNA capture probe; AAP, ascorbic acid 2-phosphate; MgO, magnesium oxide nanoflower; FcM, Ferrocene methanol; LNA, locked nucleic acid; DNA-MB, hairpin molecule beacon DNA; DenAu, dendritic gold nanostructure

Highlights

- acpcPNA probe was employed for a label-free electrochemical miRNA-21 biosensor.
- Silver nanofoam was used as stationary redox indicator and platform for probe immobilization.
- The acpcPNA biosensor showed potential for DNA, RNA and RNA mimic detection.
- The sensor provided a simple direct detection of miRNA-21 in plasma sample.
- The sensor would be potentially useful for miRNAs detection in clinical application.